Bi-allelic Mutations in *LSS*, Encoding Lanosterol Synthase, Cause Autosomal-Recessive Hypotrichosis Simplex

Maria-Teresa Romano,[1] Aylar Tafazzoli,[1] Maximilian Mattern,[1] Sugirthan Sivalingam,[1] Sabrina Wolf,[1] Alexander Rupp,[2] Holger Thiele,[3] Janine Altmüller,[3,4] Peter Nürnberg,[3,4,5] Jürgen Ellwanger,[6] Reto Gambon,[7] Alessandra Baumer,[8] Nicolai Kohlschmidt,[9] Dieter Metze,[10] Stefan Holdenrieder,[2] Ralf Paus,[11,12] Dieter Lütjohann,[13] Jorge Frank,[14] Matthias Geyer,[15] Marta Bertolini,[10,16] Pavlos Kokordelis,[1,17] and Regina C. Betz[1,17,*]

Hypotrichosis simplex (HS) is a rare form of hereditary alopecia characterized by childhood onset of diffuse and progressive scalp and body hair loss. Although research has identified a number of causal genes, genetic etiology in about 50% of HS cases remains unknown. The present report describes the identification via whole-exome sequencing of five different mutations in the gene *LSS* in three unrelated families with unexplained, potentially autosomal-recessive HS. Affected individuals showed sparse to absent lanugo-like scalp hair, sparse and brittle eyebrows, and sparse eyelashes and body hair. *LSS* encodes lanosterol synthase (LSS), which is a key enzyme in the cholesterol biosynthetic pathway. This pathway plays an important role in hair follicle biology. After localizing LSS protein expression in the hair shaft and bulb of the hair follicle, the impact of the mutations on keratinocytes was analyzed using immunoblotting and immunofluorescence. Interestingly, wild-type LSS was localized in the endoplasmic reticulum (ER), whereas mutant LSS proteins were localized in part outside of the ER. A plausible hypothesis is that this mislocalization has potential deleterious implications for hair follicle cells. Immunoblotting revealed no differences in the overall level of wild-type and mutant protein. Analyses of blood cholesterol levels revealed no decrease in cholesterol or cholesterol intermediates, thus supporting the previously proposed hypothesis of an alternative cholesterol pathway. The identification of *LSS* as causal gene for autosomal-recessive HS highlights the importance of the cholesterol pathway in hair follicle biology and may facilitate novel therapeutic approaches for hair loss disorders in general.

Rare monogenic hair loss disorders (alopecias) represent valuable models for the identification of the genes that regulate human hair follicle biology.[1–3] Clinical classification of these rare forms of alopecia is based on disease onset, affected body sites, hair shaft structure, and the involvement of organs other than the skin (syndromic alopecias). The most prevalent form of monogenic alopecia is hypotrichosis simplex (HS [MIM: 146520, 278150, 146550, 604379, 607903, 613981, 615059, 615896, and 605389]), a disorder characterized by a childhood onset of diffuse and progressive scalp and/or body hair loss. Both within and between affected families, the phenotypic spectrum of HS is highly variable, and genetic research has identified autosomal-dominant and autosomal-recessive forms of the disorder.[3–6] Over the last two decades, HS-associated mutations have been identified in a total of ten genes, with autosomal-recessive forms having shown association with mutations in *LPAR6* (MIM: 609239), *LIPH* (MIM: 607365), and *DSG4* (MIM: 607892).[7–9] Despite these breakthroughs, genetic etiology in around 50% of familial and sporadic HS cases remains unknown.

The aim of the present study was to further elucidate the genetic background of HS via whole-exome sequencing (WES). Causative mutations for autosomal-recessive HS were identified in the lanosterol synthase (*LSS*) gene (MIM: 600909), which encodes the protein lanosterol synthase (LSS; EC 5.4.99.7). LSS is implicated in cholesterol biosynthesis, thus emphasizing the key role of this metabolic pathway in the homeostasis of hair growth.

The study was approved by the ethics committee of the Medical Faculty of the University of Bonn, Germany, and all study procedures were performed in accordance with the principles of the Declaration of Helsinki. All participants provided written informed consent prior to inclusion.

The initial blood samples for the present study were collected from an affected female sib-pair of Arabic origin (Figures 1A, 1B, and S1A, individuals II:1 and II:2). DNA

[1]Institute of Human Genetics, University of Bonn, School of Medicine and University Hospital Bonn, 53127 Bonn, Germany; [2]Institute of Laboratory Medicine, German Heart Center, Technical University Munich, 80636 Munich, Germany; [3]Cologne Center for Genomics, University of Cologne, 50931 Cologne, Germany; [4]Center for Molecular Medicine Cologne, University of Cologne, 50931 Cologne, Germany; [5]Cologne Excellence Cluster on Cellular Stress Responses in Aging-Associated Diseases, University of Cologne, 50931 Cologne, Germany; [6]Dermatological Practice, 80333 München, Germany; [7]Pediatric Practice Feldstrasse, 7430 Thusis, Switzerland; [8]Institute for Genetic Medicine, University of Zürich, 8952 Schlieren, Switzerland; [9]Institute of Clinical Genetics, 53111 Bonn, Germany; [10]Department of Dermatology, University of Münster, 48149 Münster, Germany; [11]Department of Dermatology & Cutaneous Surgery, University of Miami Miller School of Medicine, Miami, FL 33136, USA; [12]Centre for Dermatology Research, University of Manchester, Manchester, UK; [13]Institute for Clinical Chemistry and Clinical Pharmacology, University of Bonn, 53127 Bonn, Germany; [14]Department of Dermatology, Venereology and Allergology, University Medical Center Göttingen, 37075 Göttingen, Germany; [15]Institute of Innate Immunity, University of Bonn, 53175 Bonn, Germany; [16]Monasterium Laboratory - Skin and Hair Research Solutions GmbH, 48149 Münster, Germany
[17]These authors contributed equally to this work
*Correspondence: regina.betz@uni-bonn.de
https://doi.org/10.1016/j.ajhg.2018.09.011.

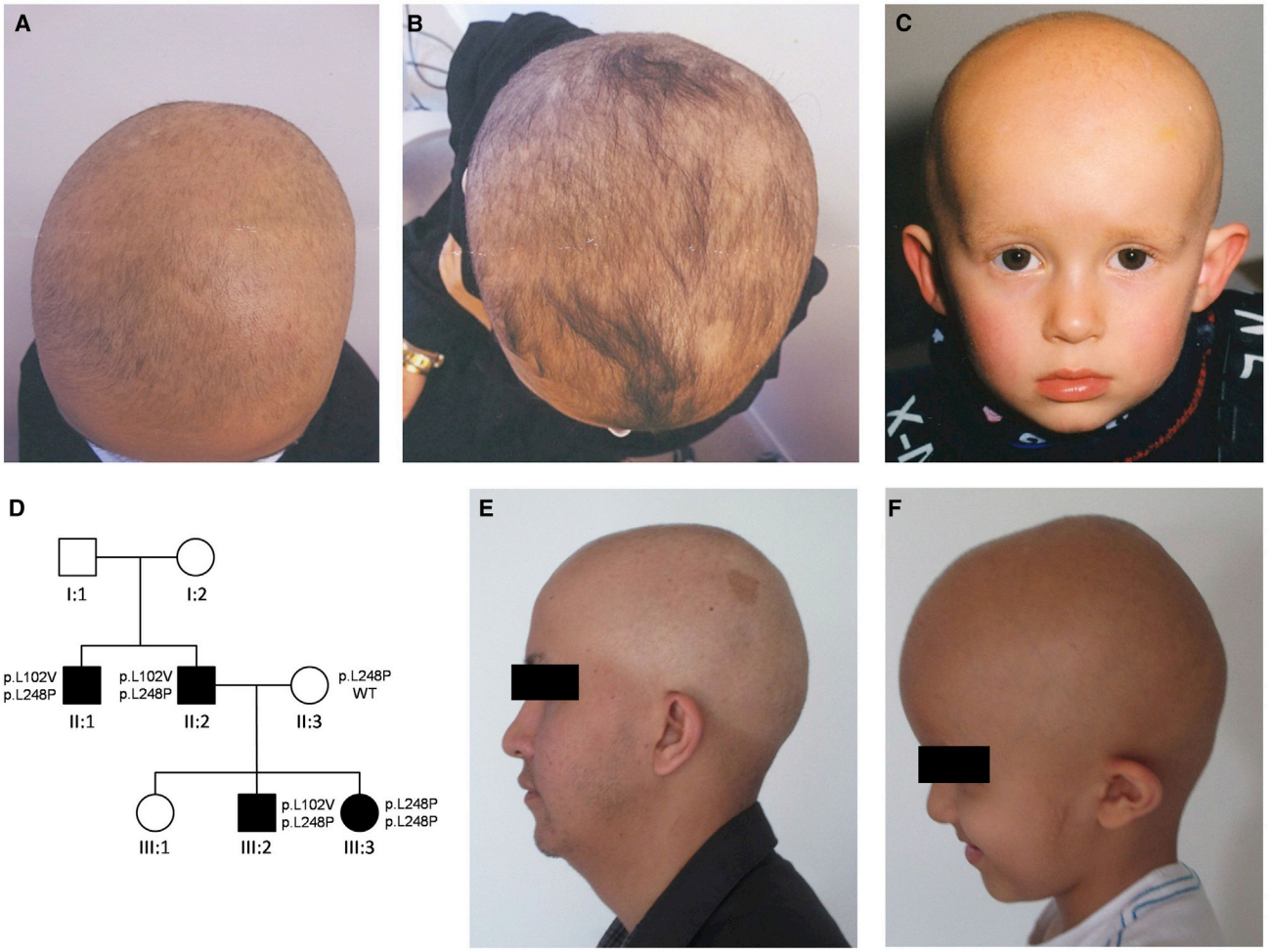

Figure 1. Clinical Features and Mode of Transmission
(A) 16-year-old female of Arabic origin (individual II:2 in Figure S1A) with sparse, lanugo-like scalp hair, and a pronounced loss of scalp hair.
(B) 19-year-old female from the same Arabic family (individual I:2 in Figure S1A) with equally reduced but slightly longer scalp hair.
(C) Index case (individual II:1 in Figure S1B) of Swiss origin at age 2 years, presenting with very sparse, lanugo-like scalp hair and sparse and brittle eyebrows and eyelashes.
(D) Pedigree of the HS family from Afghanistan demonstrates pseudodominance. Affected family members are shown in black; circles and squares denote females and males, respectively. Mutations of sequenced individuals are depicted.
(E and F) Clinical manifestation in the Afghani patients (individual II:2 and III:2 in Figure 1D): sparse scalp hair, sparse to normal eyebrows, normal eyelashes, and sparse beard hair (individual II:2).

was extracted from peripheral blood according to standard procedures. No blood samples from the unaffected parents were available.

Both sisters had presented at birth with sparse, lanugo-like scalp hair and short and brittle eyelashes. Pronounced scalp hair loss and partial loss of the eyebrows and eyelashes commenced in primary school. At the ages of 16 and 19 years, respectively, clinical examination revealed sparse scalp hair (Figures 1A and 1B) and a pronounced paucity of body hair. To investigate a suspected autosomal-recessive mode of inheritance, sequencing was performed for all genes with a known association to autosomal-recessive HS. However, no pathogenic mutation was identified. WES was then performed. First, 1 μg of DNA was sonicated, and the fragments were subjected to end-repair and adaptor-ligation. After size selection, the libraries were enriched with the SeqCap EZ Human Exome Library version 2.0 kit (Roche NimbleGen). The libraries were then sequenced using a paired end protocol and an Illumina HiSeq 2000 (Illumina), as described elsewhere.[10]

Data filtering and analysis were performed using the varbank pipeline v.2.18. These steps focused on rare autosomal variants that were present in a homozygous or potentially compound heterozygous state and shared by both sisters. In addition, different variables were considered, including (1) known phenotypes associated with candidate genes, (2) pathogenicity scores of the mutations, (3) annotation of the mutations in exome/genome sequencing databases, (4) tissue expression data, and (5) screening of the available control cohort and unrelated patients. Data analysis revealed the homozygous missense mutation c.1172T>C (p.Phe391Ser) in *LSS*

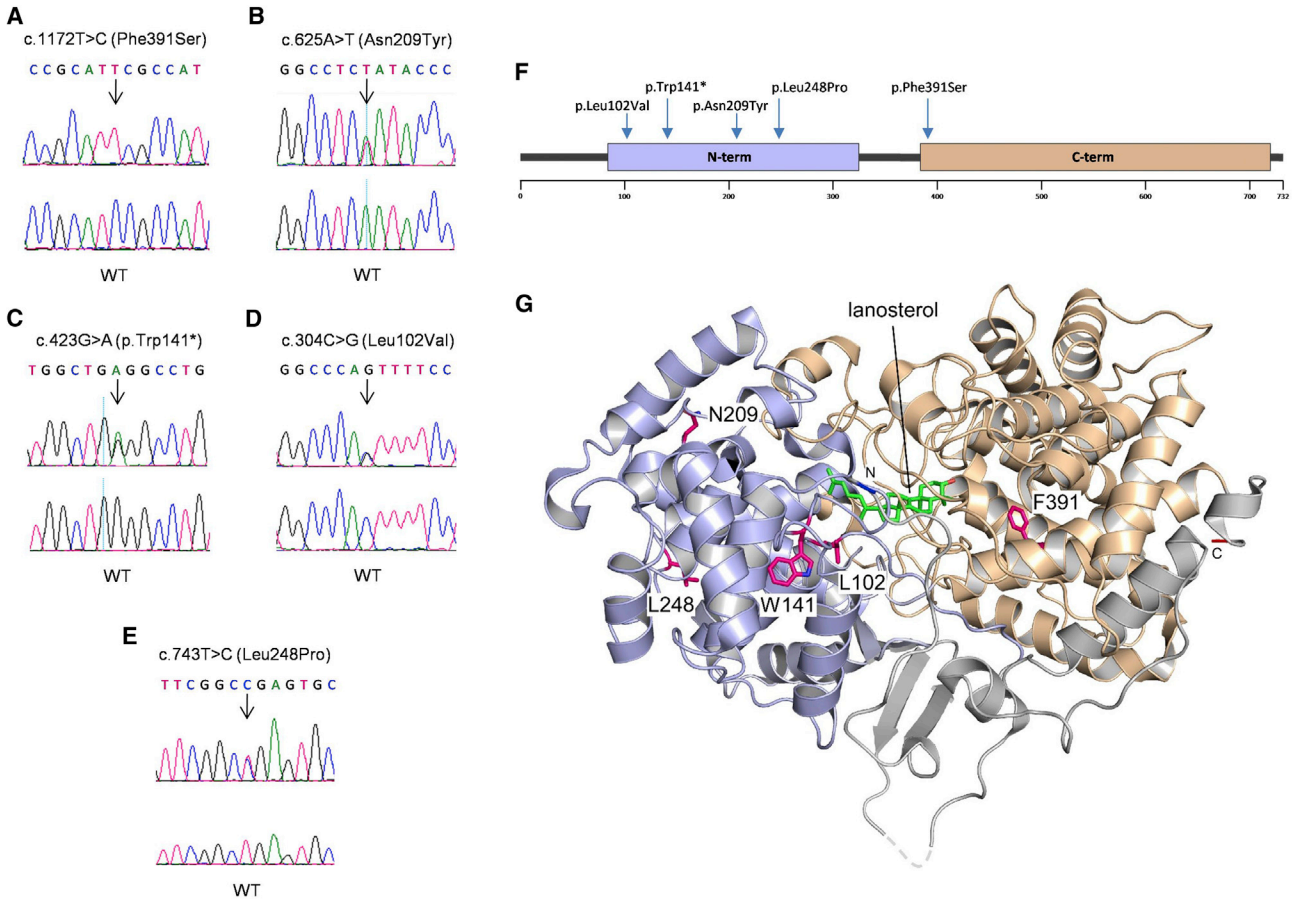

Figure 2. Sanger Sequencing, Localization of Mutations, and Structural Models
(A–E) Electropherograms of the five mutations identified in the present families, compared to the respective wild-type sequences.
(F) Schematic of the protein structure of LSS. The structure includes two major domains at the N terminus (amino acid residues 84–325) and C terminus (amino acid residues 384–720), respectively. The positions of the present five mutations are indicated.
(G) Structure of human LSS showing the helical assembly of the N- and C-terminal domains forming the active site cavity (PDB: 1W6K). The ligand lanosterol in the active site of the protein is shown. The position of the premature stop at Trp141 and the four mutant sites p.Leu102Val, p.Asn209Tyr, p.Leu248Pro, and p.Phe391Ser are indicated.

(GenBank: NM_002340.5) (Figure 2A). Other compound heterozygous mutations were excluded as none of them was in a plausible candidate gene. Thus, *LSS* was considered the only candidate, and we focused our attention on this gene. The c.1172T>C (p.Phe391Ser) *LSS* variant was confirmed by Sanger sequencing, which was performed using the BigDye Terminator v.1.1 Cycle Sequencing kit and an ABI 3100 genetic analyzer (both Applied Biosystems). Primers are listed in Table S1. Subsequent screening of the Bonn HS cohort led to the identification of *LSS* mutations in two additional families.

In a non-consanguineous family from Switzerland, a sib-pair presented with congenital alopecia (Figures 1C and S1B; individuals II:1 and II:2). On recent clinical examination in adolescence, both siblings displayed sparse, lanugo-like scalp hair, sparse and brittle eyebrows, sparse and thinned eyelashes, sparse hair on the extremities, and an absence of axillary and pubic hair (data not shown). In addition, both siblings displayed intellectual disability. In both affected individuals, mutation analysis revealed compound heterozygosity for one missense and one nonsense mutation in *LSS*. These mutations were designated c.625A>T (p.Asn209Tyr) and c.423G>A (p.Trp141*), respectively (Figures 2B and 2C). The unaffected father carried the mutation c.423G>A (p.Trp141*) in the heterozygous state. The unaffected mother was heterozygous for mutation c.625A>T (p.Asn209Tyr).

In a non-consanguineous family from Afghanistan, four individuals (II:1, II:2, III:2, and III:3; Figure 1D) presented with HS. On clinical examination at the ages of 31, 29, 6, and 1.5 years, respectively, all four individuals presented with sparse, lanugo-like scalp hair, sparse and brittle eyebrows, normal eyelashes, normal hair on the extremities, sparse pubic hair, and an absence of axillary hair (Figures 1E and 1F). Using exome data and subsequent Sanger sequencing, the following two compound heterozygous *LSS* mutations were identified in individuals II:1 and II:2: c.304C>G (p.Leu102Val) and c.743T>C (p.Leu248Pro) (Figures 1D, 2D, and 2E). Using Sanger sequencing, both mutations were identified in individual III:2. In addition, mutation c.743T>C (p.Leu248Pro) was detected in a homozygous state in individual III:3 and in a heterozygous

state in individual II:3 (Figure 1D). The inheritance pattern in this family illustrates pseudodominance.

In total, the present analyses identified five different mutations in *LSS* (Figure 2F) in three unrelated HS-affected families of distinct ethnic origins. These comprised one nonsense mutation and four missense mutations. *LSS* is located on chromosome 21q22.3. Alternative splicing results in multiple transcript variants which encode for different isoforms. Transcript variant 1 (GenBank: NM_002340) has a 37,642 bp open reading frame, comprising 22 coding exons. This open reading frame encodes the 732 amino acid membrane-bound protein LSS, which is also termed oxidosqualene cyclase.

LSS is a key enzyme within the pathway of cholesterol biosynthesis.[11] Here, LSS catalyzes the transformation of (S)-2,3 oxidosqualene to lanosterol.[12] Following this transformation, cholesterol can be synthesized via one of two independent routes, the Bloch pathway[13] or the Kandutsch-Russell pathway.[14,15] Both pathways utilize the same enzymes, but in a different order, thereby leading to the formation of different intermediates. In this context, the preferential use of either of the two pathways is tissue dependent.[16] In the skin, cholesterol is mainly synthesized via the Kandutsch-Russell pathway, which is also responsible for the formation of vitamin D from 7-dehydrocholesterol.[16,17]

Sequence deviations at amino acid residue Trp141 of LSS are not annotated in the Exome Aggregation Consortium (ExAC) or the Genome Aggregation Database (gnomAD) (Table S2). Notwithstanding, the nonsense mutation p.Trp141* is likely to result in either nonsense-mediated mRNA decay or the formation of a truncated LSS protein. Of the four missense mutations detected in the present analyses, alterations at residue Leu102 are not annotated in the ExAC or gnomAD. For the amino acid residues Asn209, Leu248, and Phe391, sequence deviations are reported at very low frequencies in the heterozygous state. However, none of the aforementioned databases describe these three residues in a homozygous state.

The missense mutations p.Leu102Val, p.Asn209Tyr, p.Leu248Pro, and p.Phe391Ser affect evolutionarily highly conserved amino acid residues (Figure S2) and are predicted by MutationTaster, SIFT, and PolyPhen-2 to be pathogenic.

The three-dimensional structure of human LSS has been determined via X-ray crystallography.[18] Analysis of the impact of the present missense mutations on LSS structure revealed that at least three of these mutations will have deleterious effects on the protein (Figures 2G and S3). Amino acid residues Asn209 and Leu248 are localized at the interface between LSS and the bilayer of the endoplasmic reticulum (ER). Alterations at these residues will likely impair anchoring, and thus the localization of the protein at the membrane. Phe391 is located at the active site cavity directly facing the dimethyl groups of the steroid A ring system. Mutation p.Phe391Ser leads to substitution of a hydrophobic, non-polar residue by a polar amino acid. Since Phe391 defines the hydrophobic cavity that is essential for ligand binding, an amino acid change at this residue is likely to compromise the ability of the protein to interact with binding partners. Leu102 has no involvement in the binding of lanosterol or lipids and does not face the ER directly. However, substitution of this amino acid may have general deleterious effects on the folding of the protein-ligand interactions by dislocating the hydrophobic L_{102}FLL motif. Phe103 and Leu104 are arranged in a helical conformation within this motif and coordinate the aliphatic side chain of the lanosterol ligand, thereby delineating this end (or the steroid opposing end) of the ligand binding cavity. Substitution of Leu102 by the smaller valine residue could displace Phe103 and Leu104 and prevent formation of the normal ligand binding cavity, thereby altering the catalytic activity of the enzyme. The nonsense p.Trp141* mutation results in a premature stop codon and thus the omission of the N- and C-terminal catalytic domains of the 83 kD protein.

To study the structural and functional consequences of the mutations, the expression of LSS in different tissues was assessed and verified using MTC cDNA panels I and II (Takara Bio Inc.) and specific primers (Figure S4A). Expression was also verified in blood and hair follicle cDNA from healthy donors (Figure S4B). These analyses revealed that the expression of LSS is ubiquitous.

To determine the precise localization of LSS in human scalp hair follicles, skin biopsies from healthy individuals were evaluated using immunohistochemistry and immunofluorescence. Following ethics committee approval (University of Luebeck, n. 06-109, 18-07-06 and University of Muenster, n. 2014-041-b-N, 22-01-14 and n. 2015-602-f-S, 3-12-15) and written informed consent, human skin scalp specimens were obtained from women undergoing cosmetic facelift surgery. As a positive control tissue, anonymized uterine tissue samples were obtained from the Department of Pathology, University of Luebeck, following appropriate ethical approval (University of Luebeck, n. 06-109, and University of Muenster, n. 2014-041-b-N). The requirement for written patient consent was waived. Sections were prepared from paraffin-embedded tissue. Immunohistochemistry revealed LSS expression in the outer root sheath and hair matrix of the hair follicle epithelium. LSS expression was more prominent in the proximal (bulb) hair follicle and outer root sheath than in the distal compartments, i.e., the infundibulum and bulge (Figures 3A–3F). LSS expression was also observed in the dermal papilla, a few cells within the connective tissue sheath, and other extra-follicular skin structures, i.e., the epidermis, sweat glands, sebaceous glands, and blood vessels. The intrinsic brown color of melanocytes precludes precise assessment of LSS expression in the hair bulb via immunohistochemistry. Therefore, immunofluorescence analyses were performed. These demonstrated that LSS was also expressed in the hair bulb and confirmed that the protein is ubiquitously expressed in human hair and skin (Figures 3G and 3H).

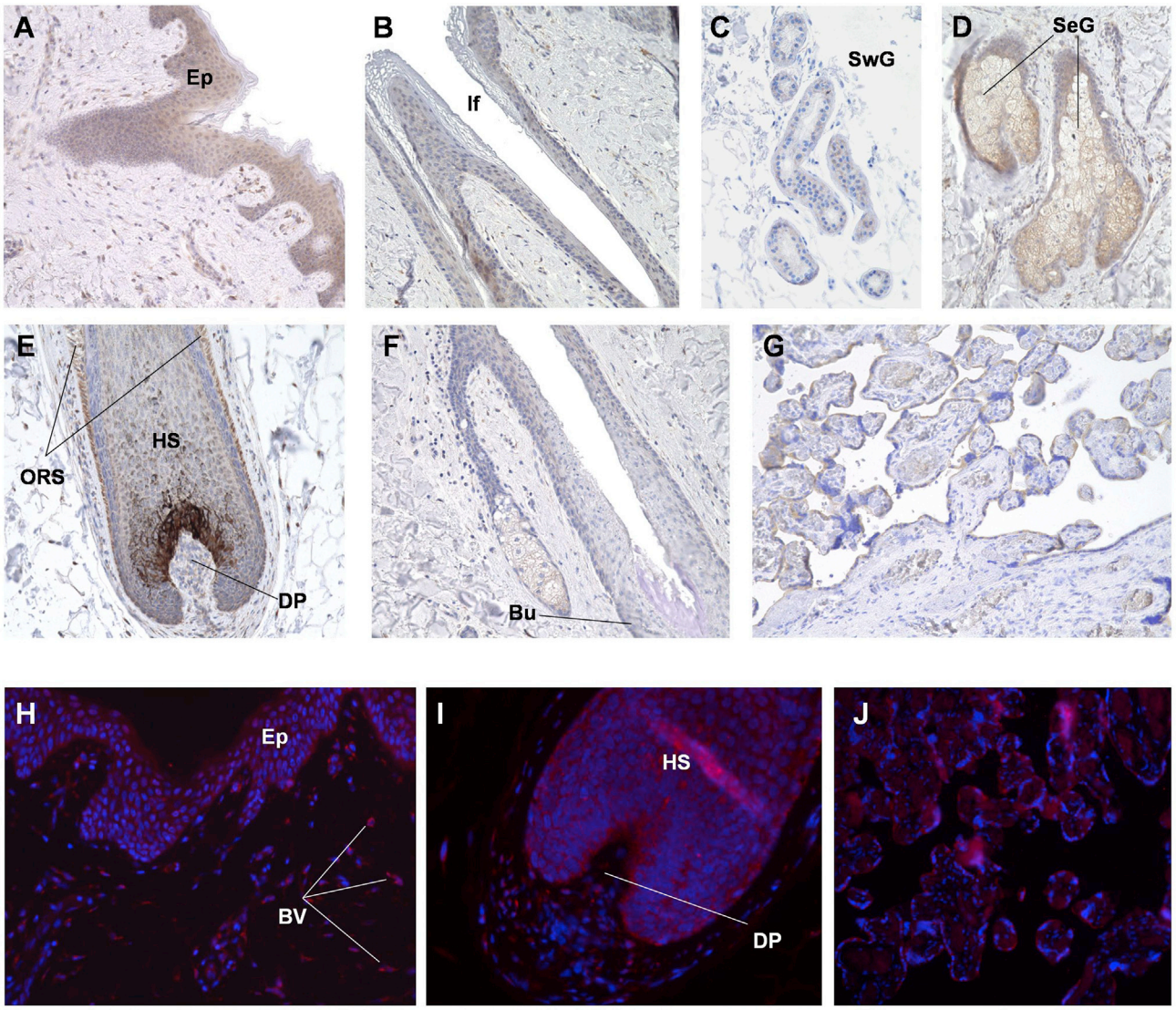

Figure 3. Immunohistochemistry and Immunofluorescence of Hair Follicle Sections and Placenta Controls

(A–G) Immunohistochemistry was performed on paraffin-embedded skin sections from healthy donors. Paraffin-embedded placenta samples were used as positive controls (G). After rehydration with xylene and decreasing concentrations of ethanol, samples were boiled in TRIS-EDTA buffer (pH 9) and treated with 3% H_2O_2. As antibodies, a rabbit monoclonal anti-LSS (ab140124; Abcam, 1:500) and a biotinilated goat anti-rabbit (111-065-003; Jackson ImmunoResearch, 1:200) were used. The Vectastain Elite ABC-HRP kit and the DAB peroxidase substrate kit (both from Vector) were used for detection. Sections were then counterstained with hematoxylin and embedded with Faramount mounting medium (Agilent Technologies).

(H–J) Prior to primary antibody incubation, immunofluorescence was carried out as described in (A). As a secondary antibody, a rhodamine goat anti-rabbit (111-025-144; Jackson ImmunoResearch, 1:200) was used. Finally, samples were stained with DAPI and embedded with Fluoromount.

Visualization with a fluorescence microscope Keyence Biozero 9000 microscope (Keyence Corporation) and Nikon lenses (Nikon) revealed a ubiquitous distribution of LSS in the skin and hair follicle. Paraffin-embedded placenta samples were used as positive controls (J). Abbreviations: Ep, epidermis; If, infundibulum; SwG, sweat gland; HS, hair shaft; ORS, outer root sheath; DP, dermal papilla; Bu, Bulge; SeG, sebaceous gland; BV, blood vessels.

Investigations were then performed to determine whether the present mutations have a differential impact on LSS protein levels. For this purpose, a pcDNA3.1 vector containing the sequence for *LSS* transcript variant 1 was used (GenScript). Using primers listed in Table S3 and the QuikChange II Site-Directed Mutagenesis kit (Agilent), specific mutants were generated. Subsequently, the keratinocyte cell line HaCaT, established by Boukamp et al.,[19] was transiently transfected with the wild-type (WT) and mutant constructs. Immunoblot analysis with an anti-LSS antibody that binds to the N terminus of the protein revealed the presence of a band of around 80 kDa for both the WT and the missense mutants (Figure 4A). Quantification of LSS revealed no significant difference in protein level, indicating that the missense mutations do not impair protein production. Although the mutation p.Trp141* is most probably pathogenic, its effect was assessed via immunoblotting. No signal was generated for

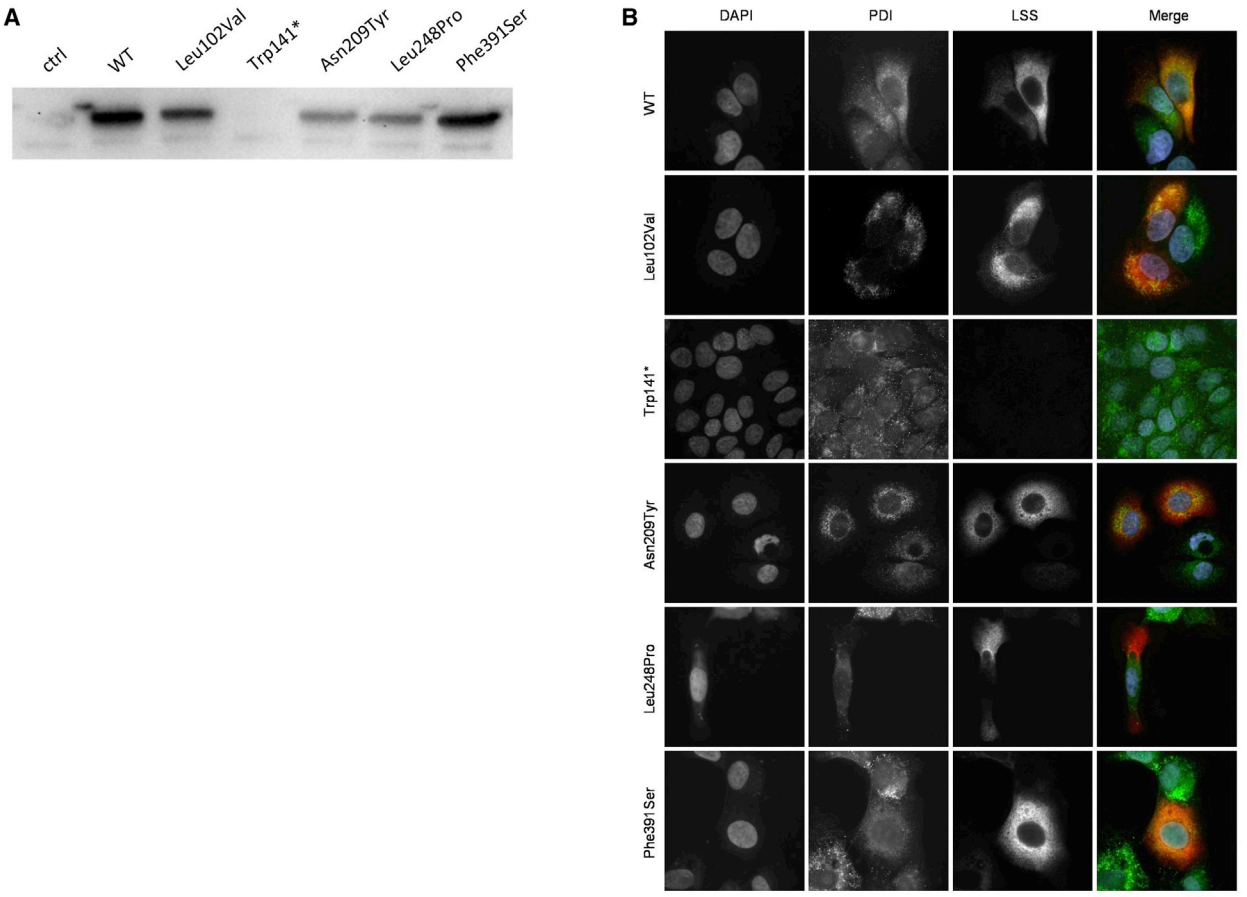

Figure 4. Immunoblot and Immunofluorescence Analyses of Keratinocyte Cells Reveal Transient Expression of Wild-Type and Mutant LSS

(A) Immunofluorescence analysis was performed in triplicates on transiently transfected HaCaT cells grown on coverslips. Cells were fixed with paraformaldehyde 4% and then permeabilized with PBS-Tween20 for 10 min. After blocking with BSA supplemented with 1% normal goat serum for 1 hr, cells were incubated with mouse monoclonal anti-LSS antibody (sc-514507; Santa Cruz, 1:500) and rabbit monoclonal anti-PDI (EPR9499; Abcam, 1:500) for an additional hour. This was followed by incubation for 40 min with the secondary antibodies anti-mouse Cy3 (A10521, LifeTechnologies, 1:500) and anti-rabbit AlexaFluor488 (ab150077, Abcam, 1:500) with addition of DAPI (Invitrogen). Slides were then mounted with Mowiol and images were generated with the Zeiss Axioplan 2 imaging microscope and the Cytovision 7.4 software. The analysis revealed the co-localization of wild-type (WT) LSS with the endoplasmic reticulum (ER). For the missense mutants, distribution of LSS both inside and outside of the ER was detected. No LSS signal was observed for the nonsense mutant.

(B) For immunoblotting, the WT LSS and the five mutant constructs were used to transiently transfect HaCat cells. The experiment was replicated a total of three times. Transfection was carried out on 60% confluent cells using Lipofectamine 3000 (Invitrogen), according to the manufacturer's instructions. After 48 hr, cells were lysed in RIPA buffer supplemented with Protease Inhibitor Cocktail (Thermo Fisher Scientific) for 30 min on ice. After sonication and centrifugation at 10,000 × *g* for 10 min, the supernatants were quantified via Bradford assay. For each sample, 40 μg of total proteins were mixed with Laemmli buffer (Bio-Rad Laboratories) and boiled at 95°C for 5 min. Samples were then run on a TGX stain-free 4%–15% precast gel and transferred to a PVDF membrane (Bio-Rad). The rest of the procedure was carried out using the mouse anti-LSS antibody (sc-514507; Santa Cruz, 1:1,000) and the WesternBreeze chemiluminescent anti-mouse kit, according to the manufacturer's instructions. Visualization of the bands and quantitation was performed with the Chemidoc imaging system and Image Lab software (Bio-Rad Laboratories). With the exception of the nonsense mutant, bands of the expected size were detected for the WT and the mutations. Quantitation was performed by normalization of the bands to total protein content in each lane. This revealed no important differences in LSS protein expression.

the mutant containing the nonsense mutation. This suggests that the transcript is unstable and rapidly degraded by nonsense-mediated mRNA decay.[20]

To study the precise cellular localization of WT and mutant LSS, immunofluorescence analyses were performed in HaCaT cells (Figure 4B). Co-staining for the protein disulfide isomerase (PDI), which is a marker for the ER, showed that WT-LSS localized to the ER. In contrast, all four missense mutants co-localized to both the ER and cytoplasm, indicating an aberrant localization pattern for mutant LSS. Therefore, a plausible hypothesis is that the present missense mutations confer their pathogenic effects through the intracellular mislocalization of mutant LSS rather than via protein-level aberrations. In accordance with the results of immunoblotting, no signal was generated for the nonsense mutation p.Trp141*. Again, this suggests that the mutant transcript undergoes rapid degradation.

To assess a possible general effect of the present *LSS* mutations on cholesterol biosynthesis, further analyses were performed in blood samples from the HS-affected family from Afghanistan (individuals II:2, II:3, III:1, and III:2; Figure 1D). Cholesterol levels and intermediates in the pathway of cholesterol biosynthesis were examined using a validated gas chromatography/mass spectrometry with selected ion monitoring approach (Supplemental Material and Methods). Hereby, we excluded blood abnormalities of cholesterol or its intermediates in affected and unaffected family members. An extended assessment of metabolites in the serum samples of this family was then performed using a metabolomic test kit and LC-MS/MS (AbsoluteIDQ p180 Kit, Biocrates Life Sciences AG). Measurements included a total of 188 metabolites. These comprised biogenic amines, amino acids, and hexoses, as well as a variety of acylcarnitines, sphingolipids, and glycerophospholipids (Supplemental Material and Methods). In accordance with the other analyses, no differences in metabolite levels were observed between homo- and heterozygote carriers.

These results suggest that the present *LSS* mutations would be expected to lead to a hair loss phenotype only. This is likely to be attributable to the presence of LSS in the cytosol and the subsequent disruption of protein-protein interactions in the endoplasmic reticulum, or a potential cellular accumulation of precursors of cholesterol synthesis.[21] This may lead to processes such as inflammation;[22] organelle stress originating in the ER, mitochondria, and peroxisomes;[23,24] or modification of lipid proteins involved in Hedgehog and Wnt signaling.[25,26] Although protein mislocalization may confer a sufficient degree of cell toxicity to cause damage to the hair follicle, it does not lead to a pathological disruption of cholesterol biosynthesis in general. In line with this hypothesis, all of the present affected individuals displayed hair abnormalities only and thus a non-syndromic form of HS, as supported by the analysis of cholesterol biosynthesis in blood and serum from the family from Afghanistan. In this context, the intellectual disability reported in the two Swiss siblings is considered coincidental. This is supported by the fact that no intellectual disability was apparent in any of the other affected individuals in the present study.

Interestingly, previous authors have reported an autosomal-recessive inheritance of *LSS* mutations in subjects with eye lens defects from China. Zhao et al. reported homozygous *LSS* mutations in two families with congenital cataracts (c.1741T>C [p.Trp581Arg] and c.1762G>A [p.Gly588Ser]).[27] In contrast to the five mutations detected in our study, the respective sequence deviations are located toward the C-terminal end of LSS, in the highly conserved terpene synthase region, where they are likely to affect the binding site for lanosterol. As in the present analyses, Zhao et al. detected no difference in cholesterol levels for WT and mutant LSS.[27] In a recent report, Chen et al. described an individual with two compound heterozygous mutations in *LSS* (c.1025T>G [p.Ile342Ser] and c.1887G>T [p.Trp629Cys]).[28] While p.Trp629Cys is even more proximal to the C terminus of LSS and downstream of the lanosterol binding site, p.Ile342Ser lies toward the N-terminal region, as do the five mutations detected in the present analyses. Interestingly, the individual reported by Chen et al. showed an intermediate phenotype, with congenital cataracts, baldness, and absent eyebrows.[28] Thus, a plausible hypothesis is that in subjects with recessive *LSS* mutations, the phenotype is dependent on the localization of the respective nucleotide change. Consequently, mutations occurring toward the N terminus of LSS would give rise to hair loss, whereas mutations toward the C terminus would be associated with ocular abnormalities.

Sterols, in particular cholesterol, are abundantly synthesized in the skin, hair follicle, and sebaceous glands and form the main components of human and animal hair.[29–31] Research has identified associations between distinct hair loss disorders in humans and mice and mutations resulting in a dysfunction of cholesterol biosynthesis. The latter involve a number of genes.[21,32–34] An unsurprising finding, therefore, is that hair loss is a reported side-effect of the statins, a group of drugs used in clinical practice to lower blood levels of cholesterol and lipids.[25]

In line with the importance of cholesterol in hair homeostasis, de Stefano et al. reported two individuals with HS secondary to mutations in *ABCA5* (MIM: 612503).[32]

This gene encodes a lipid transporter that is implicated in the efflux of cellular cholesterol.[35] The authors found that mutations in this gene resulted in an accumulation of autophagosomes and cholesterol in the lysosomes of mutant keratinocytes. Furthermore, mutations in *EBP* (MIM: 300205) cause the X-linked disorder Conradi-Hünermann-Happle syndrome (CDPX2 [MIM: 302960]), which is a variant of chondrodysplasia punctata. This syndrome is characterized by a variety of symptoms, including aberrant calcification of the bones, ichthyosis, cataracts, and alopecia. *EBP* encodes for the protein emopamil-binding protein (EBP), which is also an intermediate of cholesterol biosynthesis. The EBP protein is localized in the ER, where it functions as delta(8)-delta(7) sterol isomerase.[36] In contrast to the Afghani subjects from the present analyses, in whom blood levels of cholesterol and cholesterol biosynthesis intermediates were normal, patients with mutations in *EBP* have abnormal sterol profiles.[33] This might explain why in addition to a hair phenotype, patients with Conradi-Hünermann-Happle syndrome present with organ involvement and thus a syndromic form of alopecia, whereas the present subjects displayed a non-syndromic form of HS.

LSS plays an important role in cholesterol biosynthesis. Therefore, human *in vitro* and *in vivo* disease models based on *LSS* mutations, such as the distinct form of autosomal-recessive HS described in the present report, could have significant translational implications. In view of the demand for novel alternatives to statins,[37] the potential use of LSS as a target for cholesterol-lowering drugs is currently being

evaluated.[12,38,39] Research has shown that the inhibition of pre-squalene enzymes can impair isoprenoid biosynthesis and thus diverse vital cellular processes, such as RNA transcription, ATP synthesis, and protein modification.[38,40] Since LSS comes into play after squalene formation, this protein represents an interesting therapeutic target for the development of hypocholesterolemic drugs. However, despite this potential, no direct inhibitor of LSS has yet been approved for therapeutic use. This is probably due to the lack of selective LSS inhibitors and the putative side effects noted in pre-clinical studies. Interestingly, Pyrah et al.[41] have reported on the systemic effects of two LSS inhibitors in mice and dogs. These included the formation of cataracts in both species, while skin and hair-related defects were observed in dogs only. However, in dogs and rabbits, treatment with lanosterol prevented the formation of aggregates, thus ameliorating the cataract severity. Topical administration of lanosterol may represent a future strategy for alopecia prevention or the stimulation of hair growth.

Taken together, the present data underscore the importance of cholesterol homeostasis in the regulation of human hair biology. However, the precise mechanisms through which defective cholesterol biosynthesis leads to hair abnormalities and other pathological phenotypes, such as cataracts, remain elusive.[25] The present results suggest that perturbation of the cholesterol synthesis pathway secondary to mutations in *LSS* results in a distinct HS subtype due to mislocalization of mutant LSS in the cytoplasm. The present findings therefore suggest that LSS plays an important role in the regulation of hair growth and may facilitate the development of novel therapies for hair loss.

Supplemental Data

Supplemental Data include four figures, three tables, and Supplemental Material and Methods and can be found with this article online at https://doi.org/10.1016/j.ajhg.2018.09.011.

Acknowledgments

We thank the patients and their families for participating in this study. R.C.B. received local funding from the BONFOR program. R.C.B. and M.G. are members of the German Research Foundation (DFG)-funded excellence cluster ImmunoSensation. R.C.B. is a past recipient of a Heisenberg Professorship of the DFG (BE 2346/4-2).

Declaration of Interests

P.N. is a founder, CEO, and shareholder of ATLAS Biolabs GmbH. ATLAS Biolabs GmbH is a service provider for genomic analyses. The remaining authors have no conflicts of interest to declare.

Received: July 31, 2018
Accepted: September 22, 2018
Published: October 25, 2018

Web Resources

BLAST, https://blast.ncbi.nlm.nih.gov/Blast.cgi
ExAC Browser (accessed 5 March 2015), http://exac.broadinstitute.org/
GenBank, https://www.ncbi.nlm.nih.gov/genbank/
OMIM, http://www.omim.org/
RCSB Protein Data Bank, http://www.rcsb.org/pdb/home/home.do
UCSC Human Genome Browser, http://genome.ucsc.edu/cgi-bin/hgGateway
varbank, https://varbank.ccg.uni-koeln.de

References

1. Frank, J., Pignata, C., Panteleyev, A.A., Prowse, D.M., Baden, H., Weiner, L., Gaetaniello, L., Ahmad, W., Pozzi, N., Cserhalmi-Friedman, P.B., et al. (1999). Exposing the human nude phenotype. Nature *398*, 473–474.
2. Cichon, S., Anker, M., Vogt, I.R., Rohleder, H., Pützstück, M., Hillmer, A., Farooq, S.A., Al-Dhafri, K.S., Ahmad, M., Haque, S., et al. (1998). Cloning, genomic organization, alternative transcripts and mutational analysis of the gene responsible for autosomal recessive universal congenital alopecia. Hum. Mol. Genet. *7*, 1671–1679.
3. Betz, R.C., Cabral, R.M., Christiano, A.M., and Sprecher, E. (2012). Unveiling the roots of monogenic genodermatoses: genotrichoses as a paradigm. J. Invest. Dermatol. *132*, 906–914.
4. Levy-Nissenbaum, E., Betz, R.C., Frydman, M., Simon, M., Lahat, H., Bakhan, T., Goldman, B., Bygum, A., Pierick, M., Hillmer, A.M., et al. (2003). Hypotrichosis simplex of the scalp is associated with nonsense mutations in *CDSN* encoding corneodesmosin. Nat. Genet. *34*, 151–153.
5. Pasternack, S.M., Refke, M., Paknia, E., Hennies, H.C., Franz, T., Schäfer, N., Fryer, A., van Steensel, M., Sweeney, E., Just, M., et al. (2013). Mutations in SNRPE, which encodes a core protein of the spliceosome, cause autosomal-dominant hypotrichosis simplex. Am. J. Hum. Genet. *92*, 81–87.
6. Shimomura, Y., Agalliu, D., Vonica, A., Luria, V., Wajid, M., Baumer, A., Belli, S., Petukhova, L., Schinzel, A., Brivanlou, A.H., et al. (2010). APCDD1 is a novel Wnt inhibitor mutated in hereditary hypotrichosis simplex. Nature *464*, 1043–1047.
7. Pasternack, S.M., von Kügelgen, I., Al Aboud, K., Lee, Y.-A., Rüschendorf, F., Voss, K., Hillmer, A.M., Molderings, G.J., Franz, T., Ramirez, A., et al. (2008). G protein-coupled receptor P2Y5 and its ligand LPA are involved in maintenance of human hair growth. Nat. Genet. *40*, 329–334.
8. Kazantseva, A., Goltsov, A., Zinchenko, R., Grigorenko, A.P., Abrukova, A.V., Moliaka, Y.K., Kirillov, A.G., Guo, Z., Lyle, S., Ginter, E.K., and Rogaev, E.I. (2006). Human hair growth deficiency is linked to a genetic defect in the phospholipase gene LIPH. Science *314*, 982–985.
9. Kljuic, A., Bazzi, H., Sundberg, J.P., Martinez-Mir, A., O'Shaughnessy, R., Mahoney, M.G., Levy, M., Montagutelli, X., Ahmad, W., Aita, V.M., et al. (2003). Desmoglein 4 in hair follicle differentiation and epidermal adhesion: evidence from inherited hypotrichosis and acquired pemphigus vulgaris. Cell *113*, 249–260.
10. Ü Basmanav, F.B., Cau, L., Tafazzoli, A., Méchin, M.C., Wolf, S., Romano, M.T., Valentin, F., Wiegmann, H., Huchenq, A., Kandil, R., et al. (2016). Mutations in three genes encoding

proteins involved in hair shaft formation cause uncombable hair syndrome. Am. J. Hum. Genet. *99*, 1292–1304.
11. Mercer, E.I. (1993). Inhibitors of sterol biosynthesis and their applications. Prog. Lipid Res. *32*, 357–416.
12. Ruf, A., Müller, F., D'Arcy, B., Stihle, M., Kusznir, E., Handschin, C., Morand, O.H., and Thoma, R. (2004). The monotopic membrane protein human oxidosqualene cyclase is active as monomer. Biochem. Biophys. Res. Commun. *315*, 247–254.
13. Bloch, K. (1965). The biological synthesis of cholesterol. Science *150*, 19–28.
14. Kandutsch, A.A., and Russell, A.E. (1960). Preputial gland tumor sterols. 2. The identification of 4 alpha-methyl-Delta 8-cholesten-3 beta-ol. J. Biol. Chem. *235*, 2253–2255.
15. Kandutsch, A.A., and Russell, A.E. (1960). Preputial gland tumor sterols. 3. A metabolic pathway from lanosterol to cholesterol. J. Biol. Chem. *235*, 2256–2261.
16. Mitsche, M.A., McDonald, J.G., Hobbs, H.H., and Cohen, J.C. (2015). Flux analysis of cholesterol biosynthesis in vivo reveals multiple tissue and cell-type specific pathways. eLife *4*, e07999.
17. Prabhu, A.V., Luu, W., Li, D., Sharpe, L.J., and Brown, A.J. (2016). DHCR7: A vital enzyme switch between cholesterol and vitamin D production. Prog. Lipid Res. *64*, 138–151.
18. Thoma, R., Schulz-Gasch, T., D'Arcy, B., Benz, J., Aebi, J., Dehmlow, H., Hennig, M., Stihle, M., and Ruf, A. (2004). Insight into steroid scaffold formation from the structure of human oxidosqualene cyclase. Nature *432*, 118–122.
19. Boukamp, P., Petrussevska, R.T., Breitkreutz, D., Hornung, J., Markham, A., and Fusenig, N.E. (1988). Normal keratinization in a spontaneously immortalized aneuploid human keratinocyte cell line. J. Cell Biol. *106*, 761–771.
20. Baker, K.E., and Parker, R. (2004). Nonsense-mediated mRNA decay: terminating erroneous gene expression. Curr. Opin. Cell Biol. *16*, 293–299.
21. Serra, M., Matabosch, X., Ying, L., Watson, G., and Shackleton, C. (2010). Hair and skin sterols in normal mice and those with deficient dehydrosterol reductase (DHCR7), the enzyme associated with Smith-Lemli-Opitz syndrome. J. Steroid Biochem. Mol. Biol. *122*, 318–325.
22. Karnik, P., Tekeste, Z., McCormick, T.S., Gilliam, A.C., Price, V.H., Cooper, K.D., and Mirmirani, P. (2009). Hair follicle stem cell-specific PPARgamma deletion causes scarring alopecia. J. Invest. Dermatol. *129*, 1243–1257.
23. Murphy, S., Martin, S., and Parton, R.G. (2009). Lipid droplet-organelle interactions; sharing the fats. Biochim. Biophys. Acta *1791*, 441–447.
24. Ron, D., and Walter, P. (2007). Signal integration in the endoplasmic reticulum unfolded protein response. Nat. Rev. Mol. Cell Biol. *8*, 519–529.
25. Stenn, K.S., and Karnik, P. (2010). Lipids to the top of hair biology. J. Invest. Dermatol. *130*, 1205–1207.
26. Lewis, P.M., Dunn, M.P., McMahon, J.A., Logan, M., Martin, J.F., St-Jacques, B., and McMahon, A.P. (2001). Cholesterol modification of sonic hedgehog is required for long-range signaling activity and effective modulation of signaling by Ptc1. Cell *105*, 599–612.
27. Zhao, L., Chen, X.-J., Zhu, J., Xi, Y.-B., Yang, X., Hu, L.-D., Ouyang, H., Patel, S.H., Jin, X., Lin, D., et al. (2015). Lanosterol reverses protein aggregation in cataracts. Nature *523*, 607–611.
28. Chen, X., and Liu, L. (2017). Congenital cataract with LSS gene mutations: a new case report. J. Pediatr. Endocrinol. Metab. *30*, 1231–1235.
29. Lee, W.-S. (2011). Integral hair lipid in human hair follicle. J. Dermatol. Sci. *64*, 153–158.
30. Wertz, P.W., and Downing, D.T. (1989). Integral lipids of mammalian hair. Comp. Biochem. Physiol. B *92*, 759–761.
31. Masukawa, Y., Narita, H., and Imokawa, G. (2005). Characterization of the lipid composition at the proximal root regions of human hair. J. Cosmet. Sci. *56*, 1–16.
32. DeStefano, G.M., Kurban, M., Anyane-Yeboa, K., Dall'Armi, C., Di Paolo, G., Feenstra, H., Silverberg, N., Rohena, L., López-Cepeda, L.D., Jobanputra, V., et al. (2014). Mutations in the cholesterol transporter gene ABCA5 are associated with excessive hair overgrowth. PLoS Genet. *10*, e1004333.
33. Ikegawa, S., Ohashi, H., Ogata, T., Honda, A., Tsukahara, M., Kubo, T., Kimizuka, M., Shimode, M., Hasegawa, T., Nishimura, G., and Nakamura, Y. (2000). Novel and recurrent EBP mutations in X-linked dominant chondrodysplasia punctata. Am. J. Med. Genet. *94*, 300–305.
34. Zheng, Y., Eilertsen, K.J., Ge, L., Zhang, L., Sundberg, J.P., Prouty, S.M., Stenn, K.S., and Parimoo, S. (1999). Scd1 is expressed in sebaceous glands and is disrupted in the asebia mouse. Nat. Genet. *23*, 268–270.
35. Ye, D., Meurs, I., Ohigashi, M., Calpe-Berdiel, L., Habets, K.L.L., Zhao, Y., Kubo, Y., Yamaguchi, A., Van Berkel, T.J.C., Nishi, T., and Van Eck, M. (2010). Macrophage ABCA5 deficiency influences cellular cholesterol efflux and increases susceptibility to atherosclerosis in female LDLr knockout mice. Biochem. Biophys. Res. Commun. *395*, 387–394.
36. Moebius, F.F., Fitzky, B.U., and Glossmann, H. (2000). Genetic defects in postsqualene cholesterol biosynthesis. Trends Endocrinol. Metab. *11*, 106–114.
37. Charlton-Menys, V., and Durrington, P.N. (2007). Squalene synthase inhibitors : clinical pharmacology and cholesterol-lowering potential. Drugs *67*, 11–16.
38. Rabelo, V.W.-H., Romeiro, N.C., and Abreu, P.A. (2017). Design strategies of oxidosqualene cyclase inhibitors: Targeting the sterol biosynthetic pathway. J. Steroid Biochem. Mol. Biol. *171*, 305–317.
39. Karunagaran, S., Kavitha, R., Vadivelu, M., Lee, K.W., and Meganathan, C. (2017). Insight mechanism of the selective lanosterol synthase inhibitor: molecular modeling, docking and density functional theory approaches. Curr Comput Aided Drug Des *13*, 275–293.
40. Trapani, L., Segatto, M., Ascenzi, P., and Pallottini, V. (2011). Potential role of nonstatin cholesterol lowering agents. IUBMB Life *63*, 964–971.
41. Pyrah, I.T., Kalinowski, A., Jackson, D., Davies, W., Davis, S., Aldridge, A., and Greaves, P. (2001). Toxicologic lesions associated with two related inhibitors of oxidosqualene cyclase in the dog and mouse. Toxicol. Pathol. *29*, 174–179.